PROCEEDINGS of the
23rd International Congress on Acoustics

9 to 13 September 2019 in Aachen, Germany

Efficient evaluation of flow induced sound sources at low frequency by fast multipole BEM

Takayuki MASUMOTO[1]; Yosuke YASUDA[2]; Naohisa INOUE[3]; Tetsuya SAKUMA[4]

[1] Cybernet Systems Co., LTD. , Japan

[2] Kanagawa University, Japan

[3] The University of Tokyo, Japan

[4] The University of Tokyo, Japan

ABSTRACT

Recently, application fields of the BEM have been expanding using the fast multipole BEM (FMBEM), which is an efficient BEM solver with the application of the fast multipole method to the BEM. However, when applying the BEM to flow induced noise analyses based on Lighthill's analogy, since the number of sound sources is enormous, the processing time for sound source evaluation increases. This markedly impairs the overall computational efficiency. To solve this problem, we have been studying a method to apply the FMBEM for sound source evaluation. Specifically, the hierarchical cell structure for grouping the boundary elements was expanded to a structure including the sound sources which are widely distributed outside the boundary, and the expanded representation of the contribution from the sound sources was introduced. However, since we used the high-frequency FMBEM which is based on Rokhlin's diagonal form, it was unstable at low frequencies. In this paper, we propose a stable sound source evaluation method at low frequencies using the low-frequency FMBEM which is based on the original multipole expansions. We also show its effect on the computational load through a numerical example: a flow induced noise analysis around a side view mirror where the number of elements and sources are roughly six thousand and three million, respectively.

Keywords: Flow Induced Noise, BEM, Fast Multipole Method, Low Frequency

1. INTRODUCTION

Flow induced sound fields have been numerically analyzed mainly by methods based on acoustic analogy (1). To do this, firstly, an unsteady flow field is calculated to obtain acoustic source terms, then propagation of far-field acoustic pressure is predicted using, for example, Curle's equation (2), the Ffowcs Williams-Hawkings equation (3) or some numerical methods such as the finite element method (FEM) or the boundary element method (BEM) based on Lighthill's analogy (4, 5). Among them, the BEM is widely used for exterior sound field analyses due to several benefits such as the smart modelling capability of acoustic radiation fields and the feature of easy mesh generation. However, since dense matrices are generated in the BEM, the calculation cost for the main-process, in which the sound pressure at the boundary element nodes are calculated, becomes large especially at high frequencies. In addition, in the flow induced sound field analyses based on Lighthill's analogy, the calculation cost for the pre-process, in which the source contribution at boundary element nodes are evaluated, is also large because an enormous number of sources are generated by the analogy.

In the main-process of the BEM, to solve the finally obtained linear system, the operation count and the required amount of memory increase by $O(N_b^2)$ even using iterative methods, where N_b is

[1] masumoto@cybernet.co.jp
[2] yyasuda@kanagawa-u.ac.jp
[3] inoue@k.u-tokyo.ac.jp
[4] sakuma@k.u-tokyo.ac.jp

the number of DOFs. To reduce the cost, a fast method, in which the fast multipole method (FMM) is applied to the BEM (FMBEM), has been developed (6, 7) and is in practical use.

In the pre-process of the BEM, the operation count is $O(N_{\mathrm{b}}N_{\mathrm{s}})$, where N_{s} is the number of sources. In flow induced sound field analyses based on Lighthill's analogy, since N_{s} equals to the number of nodes in the fluid mesh, it is drastically larger than N_{b}. Therefore the operation count for the pre-process is enormous. To solve this, we have applied the FMM to sound source evaluation (8). In this method, however, because the diagonal form proposed by Rokhlin (9) was employed, the method was only applicable to calculation at high frequencies due to its well-known instability at low frequencies.

In this paper, we propose a stable method for evaluation of enormous number of sound sources at low frequencies using the low-frequency FMM which is based on the original multipole expansion theory. We also show its effect on the computational load through a numerical example.

2. CALCULATION PROCEDURES OF FLOW INDUCED NOISE USING BEM

2.1 Flow induced sound source

Lighthill's equation in the frequency domain is derived from the equation of continuity and the compressible Navier-Stokes equation as

$$(\nabla^2 + k^2)p = \frac{\partial^2 T_{ij}}{\partial \mathrm{x}_i \, \partial \mathrm{x}_j}, \tag{1}$$

$$T_{ij} = \rho v_i v_j , \tag{2}$$

where p is the sound pressure, k is the wave number, T_{ij} are the coefficients of Lighthill's stress tensor, v_i and v_j are the i-th and j-th component of the flow velocity, respectively, in the frequency domain derived by the Discrete Fourier Transform (DFT) and ρ is the air density.

The sound pressure generated by an aerodynamic sound source defined by the right hand side of Equation (1) is calculated as

$$p(\mathbf{r}_{\mathrm{o}}, \omega) = -\frac{1}{4\pi}\frac{\partial^2}{\partial \mathrm{x}_i \, \partial \mathrm{x}_j}\int_V T_{ij}\,(\mathbf{r}_{\mathrm{s}}, \omega) G(\mathbf{r}_{\mathrm{s}}, \mathbf{r}_{\mathrm{o}}) d^3\mathbf{r}_{\mathrm{s}} , \tag{3}$$

$$G(\mathbf{r}_{\mathrm{s}}, \mathbf{r}_{\mathrm{o}}) = \frac{\exp(-jk|\mathbf{r}_{\mathrm{s}} - \mathbf{r}_{\mathrm{o}}|)}{4\pi|\mathbf{r}_{\mathrm{s}} - \mathbf{r}_{\mathrm{o}}|} , \tag{4}$$

where $\mathbf{r}_{\mathrm{s}}$ and $\mathbf{r}_{\mathrm{o}}$ are the position vectors of the sound source and the observation point, respectively, j is the imaginary unit, ω is the angular velocity and $\int_V d^3\mathbf{r}_{\mathrm{s}}$ is the volume integral with respect to the source region.

2.2 Evaluation of aerodynamic sound source contribution in BEM

To analyze a sound field represented by Equation (1) using the BEM, the contribution from a sound source represented by Equation (3) is evaluated at all boundary element nodes in the pre-process. In the case of multiple sound sources existing, the contributions are evaluated for all sound sources. Hence, the operation count for the pre-process is $O(N_{\mathrm{b}}N_{\mathrm{s}})$, where N_{b} is the number of DOFs and N_{s} is the number of sources. The computational cost for this is not a major problem in many cases since generally $N_{\mathrm{s}} \ll N_{\mathrm{b}}$. However, the flow induced sound field analyses, the operation count for the pre-process is enormous due to $N_{\mathrm{s}} \gg N_{\mathrm{b}}$.

3. EVALUATION OF SOUND SOURCE CONTRIBUTION USING FMM

3.1 Outline of FMM

First, we represent the source contribution at an observation point using the multipole and the local expansions. Next, we describe a hierarchical cell structure which is introduced for efficient calculation of the contribution from a large number of sources to a large number of observation points. Finally, we describe calculation procedures.

3.1.1 Evaluation of sound source contribution using multipole/local expansions

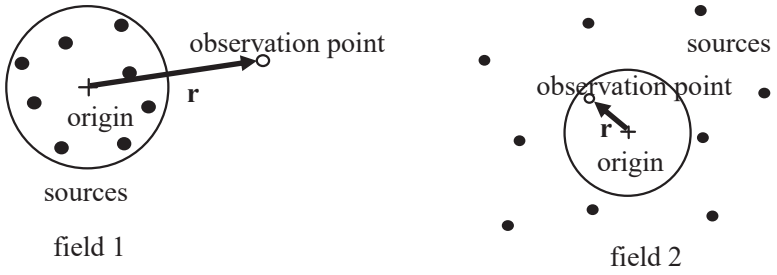

Figure 1: Illustration of two types of sound field.

Figure 1 illustrates two types of sound field, field 1 and 2. In field 1, all sources are located closer to the origin than an observation point, and the field holds the Sommerfeld radiation condition. In this case, the total contribution of source potentials at the observation point, $U(\mathbf{r})$, is represented by the multipole expansion as

$$U(\mathbf{r}) = \sum_{n=0}^{N_c-1} \sum_{m=-n}^{n} M_n^m h_n^{(1)}(kr) Y_n^m(\theta,\varphi) = \sum_{n=0}^{N_c-1} \sum_{m=-n}^{n} M_n^m S_n^m(\mathbf{r}) , \tag{5}$$

where $\mathbf{r} = (r,\theta,\varphi)$ is the position vector of the observation point in the spherical coordinate, r=$|\mathbf{r}|$, M_n^m are the multipole expansion coefficients, $h_n^{(1)}$ are the spherical Hankel functions of the first kind, Y_n^m are the spherical harmonic functions, N_c is the truncation number for infinite summation, and $S_n^m(\mathbf{r}) = h_n^{(1)}(kr)Y_n^m(\theta,\varphi)$ are the spherical wave functions of singular type. In field 2, an observation point is located closer to the origin than all source points. In this case, the total contribution of source potentials at the observation point is represented by the local expansion as

$$U(\mathbf{r}) = \sum_{n=0}^{N_c-1} \sum_{m=-n}^{n} L_n^m j_n(kr) Y_n^m(\theta,\varphi) = \sum_{n=0}^{N_c-1} \sum_{m=-n}^{n} L_n^m R_n^m(\mathbf{r}) , \tag{6}$$

where L_n^m are the local expansion coefficients, j_n are the spherical Bessel functions, and $R_n^m(\mathbf{r}) = j_n(kr)Y_n^m(\theta,\varphi)$ are the spherical wave functions of regular type.

By using these equations and by grouping the sound sources and the observation points as described below, evaluation of the contribution from the sound sources to the observation points can be replaced with that from the groups to the groups. This can reduce the operation count for the pre-process.

3.1.2 Translation of expansion coefficients

As long as the relationship illustrated in Figure 1 is satisfied, the expansion coefficients at one point, $\mathbf{r}_1$, can be translated to those at another point, $\mathbf{r}_2$, as follows:

$$\text{M2M translation: } \mathbf{M}(\mathbf{r}_2) = (\mathbf{R}|\mathbf{R})(\mathbf{t})\mathbf{M}(\mathbf{r}_1) , \tag{7}$$

$$\text{M2L translation: } \mathbf{L}(\mathbf{r}_2) = (\mathbf{S}|\mathbf{R})(\mathbf{t})\mathbf{M}(\mathbf{r}_1) , \tag{8}$$

$$\text{L2L translation: } \mathbf{L}(\mathbf{r}_2) = (\mathbf{R}|\mathbf{R})(\mathbf{t})\mathbf{L}(\mathbf{r}_1) , \tag{9}$$

where $\mathbf{M}$ and $\mathbf{L}$ are the vectors of the multipole and the local expansion coefficients, respectively, and $(\mathbf{R}|\mathbf{R})$ and $(\mathbf{S}|\mathbf{R})$ are the translation matrices for the expansion coefficients. Because those matrices are dense, their handling costs are expensive. To overcome this, we applied Rokhlin's diagonal form (9) in the previous paper (8). However, this form has a problem of instability at low frequencies. Therefore in this paper, we adopt a technique that uses the Taylor expansions for M2M and L2L translations and the rotation – coaxial translation – back rotation (RCR) technique with recurrence relations for M2L translations. Refer (7, 10) for more detail.

3.1.3 Hierarchical cell structure

A hierarchical cell structure is introduced for multilevel grouping of sources and observation points. Figure 2 shows an example in two dimensions. A cube circumscribing whole sources and observation points is created as a root cell, whose hierarchical cell level $l = 0$. Then it is divided

into eight child cubes, whose cell levels l are 1. Each divided cube is again divided recursively, whose hierarchical cell levels l are $2, 3, \cdots, L$.

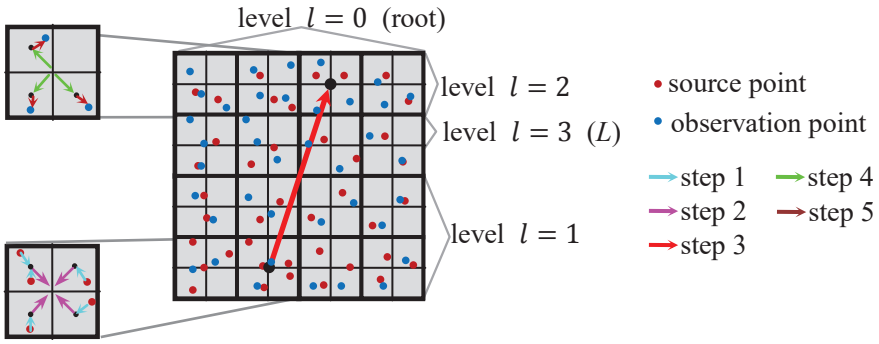

Figure 2: 2-D hierarchical cell structure and diagram of steps 1 to 5.

3.1.4 Calculation procedures

The calculation procedures to evaluate the source contribution at observation points using the expansion coefficients and the hierarchical cell structure are as follows:

Step 1: In each cell at the lowest level, the contribution of sources belonging to the cell is translated to the multipole expansion coefficients at the center of the cell, and those are accumulated.

Step 2: The multipole expansion coefficients of child cells are translated to those at the center of its parent cell, and those are accumulated.

Step 3: The multipole expansion coefficients are translated to the local expansion coefficients at the center of the distant cells at the same hierarchical cell level.

Step 4: The local expansion coefficients of the parent cell are translated to that at the center of its child cells.

Step 5: In each cell at the lowest level, the local expansion coefficients are translated to the source contribution at the observation points.

Step 6: In each cell at the lowest level, the contribution of sources belonging to its neighbor cells are evaluated in the conventional way.

3.2 FMM application to main-process of BEM

Figure 3 shows an example of the hierarchical cell structure for a boundary element mesh, which is used for the main-process of the BEM. The whole mesh is circumscribed by the root cell whose hierarchical cell level $l = 0$. The child cells are generated as described in 3.1.3.

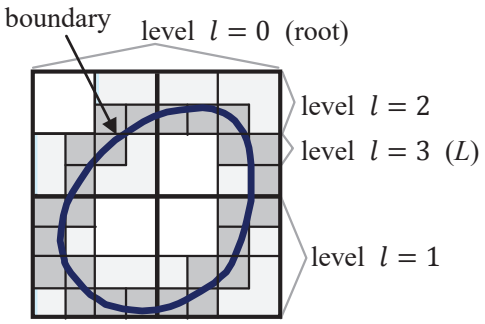

Figure 3: 2-D hierarchical cell structure (the lowest cell level $L = 3$) for main-process of BEM.

3.3 FMM application to pre-process of BEM

3.3.1 Hierarchical cell structure

When the exterior sound field excited by aerodynamic sound sources is analyzed, sound sources usually exist outside of the boundary element mesh. Hence, we generate a new hierarchical cell structure circumscribing whole sources. In order to use the coefficients of the cell structure for the main-process effectively, the higher level cells, $l = -1, -2, \cdots$, are defined recursively based on the level 0 cell until the whole sources are circumscribed by one of a newly generated cells, which is the highest level, H, cell (Figure 4).

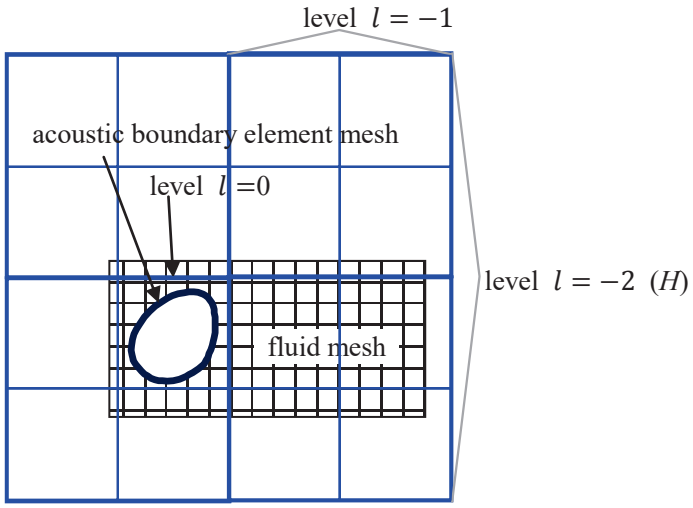

Figure 4: 2-D hierarchical cell structure (the highest cell level $H=-2$) for pre-process of BEM.

3.3.2 Calculation procedures

To begin with, we define acoustic cells. These are the cells containing acoustic boundary elements among lowest level cells, and, the higher level cells which contain acoustic cells in its child cells are also acoustic cells.

First, the processes of step 1 are executed in all the lowest level cells. Next, the processes of step 2 are recursively executed until $l=H+2$ $(l=L-1, L-2, \ldots, H+3, H+2)$. Then, at each cell level, the processes of step 3 are executed from all the cells to the acoustic cells. After that, the processes of step 4 are executed in the acoustic cells from $l=H+2$ to $l=L-1$, and the processes of step 5 are executed in the lowest level acoustic cells. Finally, the processes of step 6 are executed. Figure 5 shows an example of coefficient translation flows in the case $H=-1$ and $L=3$.

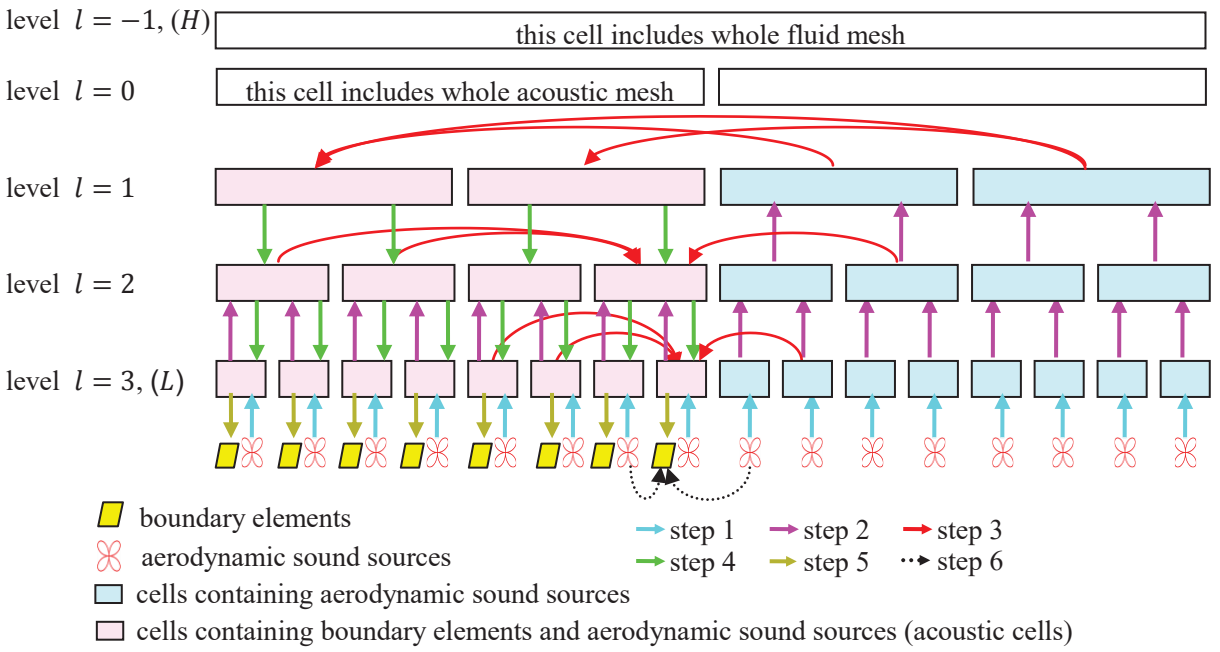

Figure 5: Conceptual diagram of translation of aerodynamic sound source contributions.

(The lowest cell level L is 3 and the highest level $H=-1$. Note that some operations in step 3 at levels 2 and 3, and step 6 at the lowest level L are omitted to be illustrated for simplicity.)

Among the FMM processes for the pre-process, only the equation evaluated in step 1 is different from that for the main-process. In step 1 of the FMM for the pre-process, the following equation is evaluated

$$M_{n\ (m_L)}^{m} = jk \sum_{l \in G_{m_L}} \sum_{i=1}^{3} \sum_{j=1}^{3} \int_V \frac{\partial^2}{\partial x_i \partial x_j} T_{ij}(\mathbf{r}_s, \omega) R_n^{-m}(\mathbf{r}_{\lambda s}) d^3\mathbf{r}_s \,, \tag{10}$$

where G_{m_L} is the group of sources included in the cell m_L, $\mathbf{r}_s$ is the position vector of the source, $\mathbf{r}_{\lambda s}$ is the vector connecting the center of the cell m_L and the source position.

4. Numerical example – side view mirror model –

4.1 Transient fluid dynamics simulation

The turbulence vortex shedding from a side view mirror, whose geometry was a half of a cylinder with a quarter sphere on its top having a diameter of 0.2 m and a height of 0.3 m, was analyzed at Reynold's number, *Re*, being 532,608 and mach number, *M*, being 0.11441 (140 km/h). As a computational fluid dynamics code, ANSYS Fluent version 15.0 (11) and its incompressible LES (Dynamic Smagorinsky model) calculation feature was used. There were 3,538,170 cells and 2,927,466 nodes in the computational domain. A steady velocity was imposed on the inflow boundary. No-slip conditions were applied on the mirror and the plate. Slip-conditions were applied on the top and the side boundaries. On the other boundary, a zero pressure outflow condition was applied. The transient simulation was performed with the time step size being 1E-4 s. Figure 6 shows a geometry and a result, which is an instantaneous snapshot of the fluid pressure.

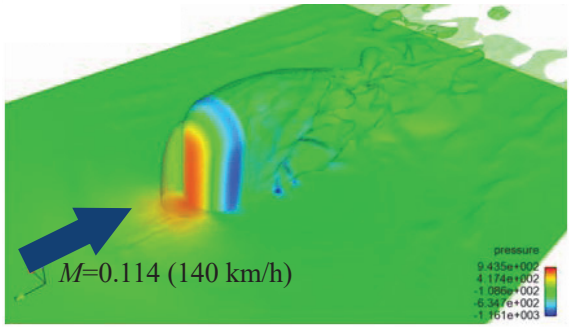

Figure 6: Instantaneous snapshot of the fluid pressure.

4.2 Acoustic simulation

The numbers of boundary elements and aerodynamic sound sources were 10,442 and 2,927,466, respectively. In a hierarchical cell structure for the pre-process, the highest hierarchical cell level, *H*, was set to -2 to circumscribe the fluid mesh, and the lowest hierarchical cell level, *L*, was varied from 3 to 7 to investigate its effect on the computational cost. For the main-process, the lowest hierarchical cell level, *L*, was selected as the average number of elements in the cell, *M*, falling below 100 first to minimize the calculation time based on the study in (7). Responses were calculated at 100 Hz by the conventional method (the direct evaluation of the sources) and the proposed method. Figure 7 shows the acoustic pressure distribution on the boundary element mesh.

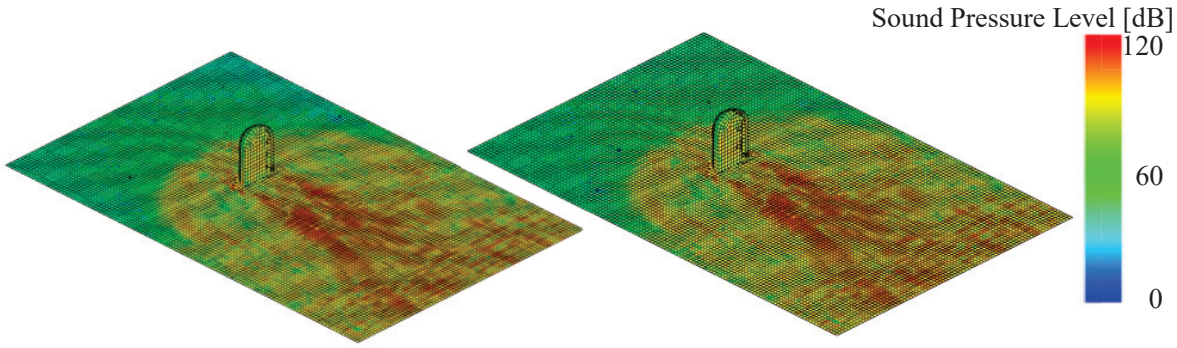

Figure 7: Acoustic pressure distribution at 100 Hz.

Left: conventional method, Right: proposed method.

In order to evaluate the difference between these two results, an error defined by the following equation was calculated and shown in Table 2

$$\varepsilon = \frac{1}{n}\sum_{i=1}^{n}\frac{\left|p_{\mathrm{C},i} - p_{\mathrm{P},i}\right|}{\max_i\left(\left|p_{\mathrm{C},i}\right|\right)}, \tag{11}$$

where n is the number of elements, $p_{\mathrm{C},i}$ and $p_{\mathrm{P},i}$ are the pressure at i-th element calculated by the conventional method and proposed method, respectively. The error did not depend on L and was enough small.

4.3 Computational cost

Table 2 also lists the computational time and required memory for the pre-process of the BEM.

The computational time for step 1 did not depend on L, because the operation count of step 1 is $O(N_{\mathrm{s}})$. Since the number of sources which are directly evaluated in step 6 decreased with an increase in L, the computational time for step 6 decreased with an increase in L, and conversely the computational time for setup and steps 2 to 5 increased with L. The optimum lowest cell level L for minimum computational time was 6 in this case. The required amount of memory increased simply with the increase in L, because no additional memory is required by the direct evaluation of the source contribution.

Table 2: Computational time and required memory for source evaluation and error in results calculated by proposed method.

(Num. of aerodynamic sound sources: 2,927,466, and num. of boundary elements: 10,442)

	M	computational time [s]					memory	error ε
		setup	step 1	steps 2-5	step 6	total	[GB]	
conventional	-	-	-	-	-	10943.8	-	-
L=3	1462	1.42	191.9	0.1	780.3	973.8	1.33	6.0E-5
L=4	238	1.86	191.4	0.8	185.4	379.5	1.40	6.0E-5
proposed L=5	45	2.43	193.2	4.2	50.9	250.8	1.74	6.0E-5
L=6	11	3.31	191.7	17.7	25.2	238.0	3.11	6.0E-5
L=7	3	5.26	192.6	62.0	10.38	270.2	7.74	8.2E-5

5. SUMMARY

We have proposed a fast method to evaluate the contribution from a large number of sound sources using the low frequency FMM. This method is especially required in the pre-process of the BEM when analyzing the flow induced sound field based on Lighthill's acoustic analogy because the number of sources in this case is large. The following points were confirmed through the numerical

analysis.

i. Sound fields calculated by the conventional and the proposed method agreed well.
ii. The computational time varied depending on the lowest hierarchical cell level, *L*. The optimum *L* which minimizes the calculation time was confirmed to exist.
iii. The memory requirement increased with *L*.
iv. The shortest computational time by the proposed method was 46 times shorter than that of the conventional method in our numerical experiment.

REFERENCES

1. Wagner C, Hüttl T, Sagaut P. Large-Eddy Simulation for Acoustics. Cambridge University Press, New York,USA; 2007.
2. Curle N. The influence of solid boundaries on aerodynamic sound. Proc Roy Soc. 1955; A231:505-514.
3. Ffowcs, Williams JE, Hawkings DL. Sound generation by turbulence and surfaces in arbitrary motion. Philosophical Transactions of the Royal Society. 1969; A264:321-342.
4. Lighthill M. On sound generated aerodynamically, I. General theory. Proc Roy Soc. 1952; A211:564-587.
5. Lighthill M. On sound generated aerodynamically, II. Turbulence as source of sound. Proc Roy Soc. 1954; A 222:1-32.
6. Sakuma T, Yasuda Y. Fast multipole boundary element method for large-scale steady-state sound field analysis. Part 1: Setup and Validation. Acta Acust united Ac. 2002; 88(4):513-525.
7. Yasuda Y, Oshima T, Sakuma T, Gunawan A, Masumoto T. Fast multipole boundary element method for low-frequency acoustic problems based on a variety of formulations. J Comput Acoust. 2010;18(4):363-395.
8. Masumoto T, Gunawan A, Mori M, Yasuda Y, Oshima T, Sakuma T. Efficient calculation for evaluating vast amounts of quadrupole sources in BEM using fast multipole method. Proc ICA 2016; 5-9 September 2016; Buenos Aires, Argentina 2016. ICA2016-309.
9. Rokhlin V. Diagonal forms of translation operators for the Helmholtz equation in three dimensions. Appl. and Comput. Harm. Anal. 1993;1:82-93.
10. Gumerov NA, Duraiswami R. Fast multipole methods for the Helmholtz equation in three dimensions. Oxford, UK;2004
11. ANSYS Fluent version 15.0 User's Guide, ANSYS Inc.